J Electroceram (2006) 17:255–261
DOI 10.1007/s10832-006-7722-1

Control of crystal polarity in oxide and nitride semiconductors by interface engineering

M. W. Cho · T. Minegishi · T. Suzuk · H. Suzuki · T. Yao · S. K. Hong · Hyunchul Ko

Received: 26 June 2005 / Revised: 18 January 2006 / Accepted: 10 February 2006
© Springer Science + Business Media, LLC 2006

Abstract The ZnO-based oxide and GaN-based nitride semiconductors have been explored for applications to photonic devices in the UV wavelength region and high power electronic devices, where the control of crystal polarity is one of the key issues. This paper will deal with the control of crystal polarity in ZnO/GaN heterostructures and ZnO/sapphire heterostructures by interface engineering.

Keywords Nitride material · Oxide material · Polarity

1 Introduction

Wide bandgap materials like GaN and ZnO are used to fabricate short-wavelength light emitters [1] and high-electron-mobility transistors [2]. Especially, ZnO is an attractive material for high efficiency ultraviolet laser and light emitting diodes, because of a direct band gap (3.37 eV) with a large excitonic binding energy (60 meV). Excitonic lasing from ZnO at room temperature has been reported [3, 4], and excitonic-stimulated emission have been observed at temperatures up to 550°C [5]. Recently, III-nitrides have promoted great advances in LEDs. High efciency GaN-based LEDs attract great interest for applications such as displays, traffic signals, back light for Liquid crystal display (LCD) and white-light sources.

Those devices have been mostly fabricated on c-sapphire substrates. Since the lattice mismatch between c-sapphire/GaN (0001) and c-sapphire/ZnO (0001) is as large as 15% and 18%, respectively, GaN and ZnO epilayers directly grown on c-sapphire contain tremendous number of defects [6]. The primary role of a buffer layer inserted in between GaN or ZnO and a c-sapphire substrate is crucial to improve crystal quality of these epilayers.

In GaN epitaxy, the control of crystal polarity of GaN epilayers is very important, since Ga-polar GaN films show better crystal quality [7], electrical and optical properties than N-polar GaN [8, 9]. The growth of Ga-polar GaN layers has been achieved using AlN buffer layers [9]. Wurtzite ZnO is considered to be an appropriate template for wurtzite GaN epitaxy, since lattice mismatch between GaN and ZnO is as small as 1.8%. High-quality ZnO layers with O polarity can be grown on c-sapphire with a thin MgO buffer layer by plasma-assisted molecular-beam epitaxy (P-MBE) [10].

ZnO has crystal polarity, Zn-polar and O-polar, and controlling polarity is an important factor for designing optical devices due to the piezo electric field and spontaneous polarization field. Impurity incorporation is dependent on crystal polarity [11]. We have employed a very thin MgO buffer layer to grow high quality ZnO thin films on c-Al_2O_3 substrate using P-MBE [12]. ZnO thin films grown on c-Al_2O_3 substrate using a few monolayer thick MgO buffer were always O-polar [13], which is the same as for ZnO directly grown on c-Al_2O_3 [14].

M. W. Cho (✉) · T. Minegishi · T. Suzuk · H. Suzuki · T. Yao
Institute for Materials Research, Tohoku University, 2-1-1 Katahira, Aobaku, Sendai 980-8577, Japan
e-mail: mwcho@cir.tohoku.ac.jp

T. Yao
Center for Interdisciplinary Research, Tohoku University. Aramaki, Aoba-ku, Sendai, 980-8578, Japan

S. K. Hong
Dept of Materials Science and Engineering, Chungnam National University, Daejeon 305-764, Korea

H. Ko
Department of Electrical and Computer Engineering, University of South Alabama, 307N. University Blvd., Mobile, Alabama 36688, USA

In this paper, we report the successful growth of Ga-polar GaN epilayers on O-polar ZnO templates pre-deposited on c-plane sapphire by NH_3 pre-exposure onto ZnO templates. Also, we will show that the crystal structure of MgO buffer varies with thickness and that the crystal polarity of ZnO layers grown on MgO buffer is controlled by only changing the MgO buffer layer thickness. Possible atomic configurations of the ZnO/MgO/Al_2O_3 interface are discussed.

2 Experimental

ZnO films used for templates were grown on c-sapphire substrates by oxygen plasma-assisted MBE using a MgO buffer. After the growth of a ZnO template, reflection high-energy electron diffraction showed a streaky pattern with the bright specular spot, which is indicative of a smooth surface. The root mean square (rms) value of the surface roughness measured by atomic force microscopy (AFM) was less than 1 nm over a 5 μm × 5 μm area. The details of the growth procedures for ZnO can be found elsewhere [10]. The growth of GaN epilayers was carried out on such ZnO(∼1.3 μm)/MgO(∼3 nm)/c-sapphire templates by ammonia-assisted MBE, where solid Ga and NH_3 gas were used as Ga and N sources, respectively. The substrate temperature for GaN growth was 800°C and the growth rate of GaN was ∼1 μm/h, in which the Ga beam pressure was 2.8×10^{-7} Torr, and NH_3 flow rate was 10 sccm. Prior to GaN growth, NH_3 was exposed onto the ZnO template at 800°C to grow a Zn_3N_2 layer, which should allow the growth of Ga-polar GaN on O-polar ZnO. In order to investigate the polarity of GaN layers grown on ZnO templates, we etched the surface of GaN, since Ga-polar is extremely harder to etch compared to N-polar GaN [15]. In order to confirm the polarity of both GaN and ZnO layers, we have used convergent beam electron diffraction (CBED) technique. The CBED experiments were performed using JEM-2010 (JEOL Ltd.) at 100 keV. The CBED patterns were obtained with a 20 nm probe for several parts of the sample. Experimental CBED patterns from ZnO and GaN layers were compared with simulated patterns [16].

ZnO/MgO/c-Al_2O_3 structure thin films were grown by plasma assisted molecular beam epitaxy (P-MBE). c-Al_2O_3 substrates were degreased in acetone, methanol for 10 min and then etched in H_2SO_4 :H_2PO_4 = 3:1 for 10 min at 160°C, followed by rinse in de-ionized water. The cleaned substrates were mounted on a substrate holder and then loaded into the MBE chamber. Conventional effusion cells were used to evaporate elemental Zn and Mg. Atomic Oxygen was generated from O_2 gas by an rf-plasma cell with power fixed at 250 W and a flow rate of 2.0 sccm. c-Al_2O_3 substrates were thermally cleaned at 800 °C for 30 min in a preparation chamber. The c-Al_2O_3 substrate was loaded into the growth chamber, following by thermal cleaning at 850°C for 10–30 min. Thermally cleaned c-Al_2O_3 substrates were exposed to O-plasma to make the surface of c-Al_2O_3 substrates O-terminated [17]. Following the substrate treatment, 0.8–5 nm thick MgO buffer layers were grown at a substrate temperature (T_{sub}) and Mg-flux (J_{Mg}) of 570°C and 0.01–0.03 Å/s, respectively. ZnO layers were grown on MgO/c-Al_2O_3 templates at a Zn-flux (J_{Zn}) of 2.0 Å/s and T_{sub} of 800°C employing a low temperature (LT-) ZnO buffer layer at J_{Zn} of 0.1 Å/s and T_{sub} of 570°C followed by subsequent annealing at T_{sub} of 850–900°C.

The Polarity of these samples was characterized by wet etching using trifluoroacetic acid (3 vol.%, 0°C) and convergent beam electron diffraction (CBED). The growth evolution of MgO buffer layers was observed with reflection high energy electron diffraction (RHEED). The interface structure of ZnO/MgO/c-Al_2O_3 was investigated by high-resolution transmission electron microscopy (HRTEM). Grazing incident X-ray diffraction (GIXRD) was carried out to characterize the epitaxy relationship, and to measure lattice constants.

3 Results and discussion

3.1 Polarity control of GaN on ZnO template substrate

3.1.1 Surface morphology and etching rate

Figure 1(a) shows an AFM image of an as-grown GaN surface. The rms surface roughness value is 23.8 nm. Etching of the GaN was performed in 0.5 M KOH(10%) solution. Figure 1(b) shows an AFM image of the GaN epilayer after etching. We note that the GaN surface morphology shows only slight change. Additionally, the etching rate of GaN is less than 0.1 nm/min which is very slow compared to typical etching rate (3.9 nm/min) of a N-polar GaN layer. These results suggest that GaN grown on NH_3-treated ZnO templates has Ga polarity.

3.1.2 Polarity characterized by CBED

CBED techniques have been widely used to determine the polarity of a wurtzite-structure material [18, 19]. When polarity is inverted, the symmetry of a CBED pattern along the *c*-axis is inverted. Figures 2(a) and (b) show simulated CBED patterns of (a) O-polar ZnO and (b) N-polar GaN obtained for a thickness of 26 nm with the zone axis of [11–20]. Since both GaN and ZnO have the same crystal structure with almost the same lattice constant, the simulated CBED pattern for O-polar ZnO and N-polar GaN should show similar patterns. Figures 2(c) and (d) show measured CBED patterns with the same zone axis of the (c) ZnO template and (d) GaN layer from a GaN/ZnO/c-sapphire specimen.

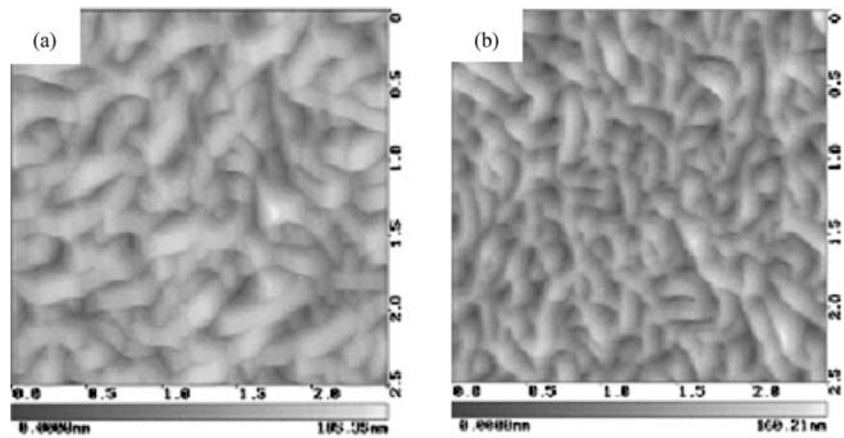

Fig. 1 AFM images of (a) an as-grown GaN epilayer grown on an NH_3 treated ZnO template, and (b) after etching in 0.5 M KOH (10%) solution for 60 min. The scan area is 2.5 μm×2.5 μm

By comparing the simulated CBED pattern of O-polar ZnO with the measured one (Figs. 2(a) and (c)), we confirm that the ZnO template has O polarity. The measured CBED pattern of the GaN (Fig. 2(d)) unequivocally show that the GaN layer has Ga polar through a comparison with the simulated CBED pattern of N-polar GaN (Fig. 2(b)). Thus, we have succeeded in growing Ga-polar GaN on an O-polar ZnO template by pre-exposure of NH_3 onto the ZnO template. Based on these experimental results, we discuss the bond sequence at the interface of Ga-polar GaN/O-polar ZnO. Figure 3 shows schematic diagrams of Ga-polar GaN and O-polar ZnO with a Zn_3N_2 interface layer in between. It is likely that the NH_3 pre-exposure onto ZnO surface induced the formation of a Zn_3N_2 interface layer. Since Zn_2N_3 has a cubic structure with a space group of Ia3, it possesses inversion symmetry. Such an interface layer with inversion symmetry can invert crystal polarity [20]. Since the (1 1 1)Zn_3N_2 plane is composed of Zn atoms, we tentatively propose a bond sequence of ...–Zn–O–(Zn–Zn_2N_3–Zn)–N–Ga– ..., which can invert the crystal polarity from anion polar to cation polar.

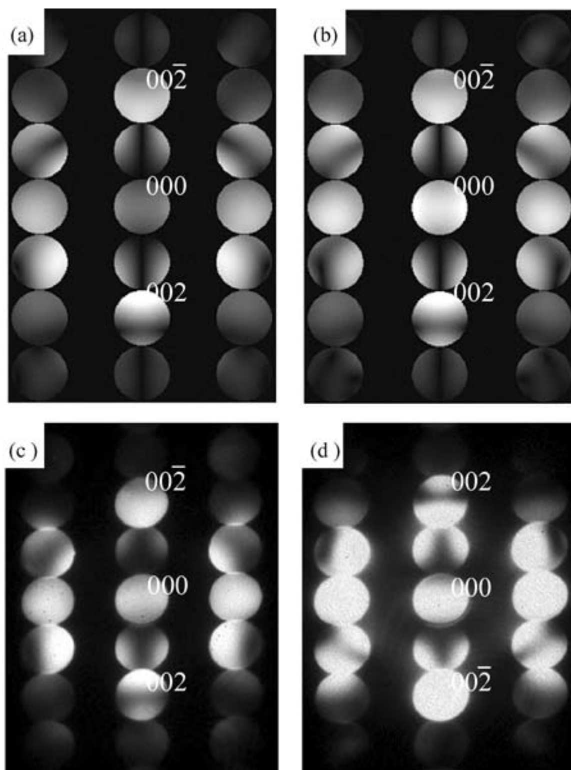

Fig. 2 Simulated CBED patterns of (a) O-polar ZnO (thickness: 26 nm) and (b) N-polar GaN (thickness: 26 nm). The measured CBED patterns of (c) ZnO template and (d) GaN layer, respectively. The zone axis is [11–20]

3.2 Polarity control of ZnO on MgO buffer layer

3.2.1 Growth and characterization of ZnO/MgO/Al_2O_3

We observed the growth evolution of the MgO buffer layer using RHEED as shown in Fig. 4. Initially, the MgO buffer layer grew 2-dimensionally on c-Al_2O_3 substrate as indicated by a streaky RHEED pattern (Fig. 4(a)). After the growth of 0.8 nm thick MgO layer, the growth mode changes from 2-dimensional to 3-dimensional, as shown by an elongated streaky RHEED pattern (Fig. 4(b)). When the MgO

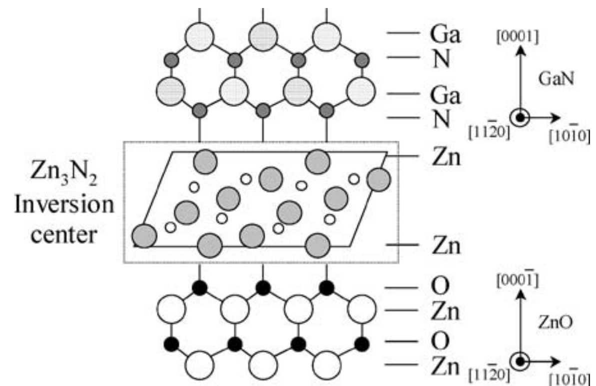

Fig. 3 Schematic diagram for bond sequence at a Ga-polar GaN/O-polar ZnO interface, where NH_3 was pre-exposed onto the O-polar ZnO prior to GaN growth

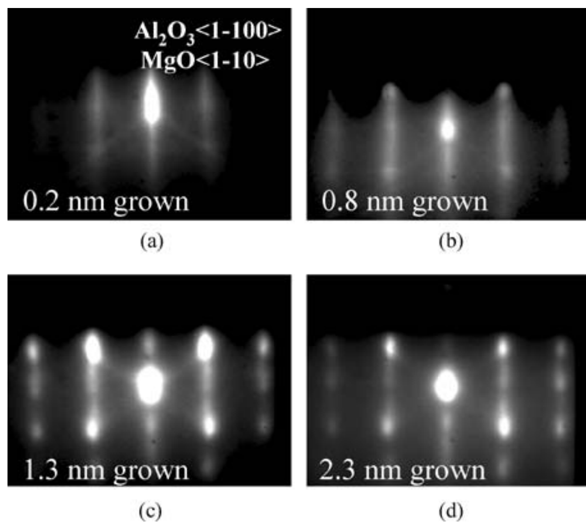

Fig. 4 The evolution of RHEED pattern during growth of MgO buffer layer. (a) The thickness of the MgO buffer layer is 0.2 nm. 2-dimensionally growth on c-Al_2O_3 as indicated by a streaky pattern. (b) $t_{MgO} = 0.8$ nm. The growth mode of MgO buffer layer changed from 2-dimensional to 3-dimensional. (c) $t_{MgO} = 1.3$ nm. Extra spots appear due to 3D growth (d) $t_{MgO} = 2.3$ nm

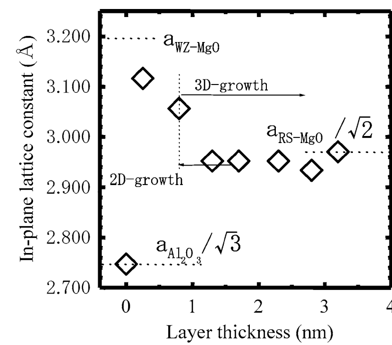

Fig. 5 Plot of in-plane lattice constant of MgO buffer layer against layer thickness estimated from RHEED pattern

thickness exceeds about 1.3 nm, extra RHEED spots appear (Fig. 4(c)), which suggests that the crystal structure of the MgO buffer layer changes with increasing layer thickness. A spotty RHEED pattern was preserved for thicker MgO layers (Fig. 4(d)).

The in-plane lattice constants of the MgO buffer layer were estimated from RHEED pattern and plotted against MgO buffer thickness in Fig. 5. When the MgO layer thickness is 0.3 nm, the in-plane lattice constant measures 0.312 nm, which is very close to the lattice constant (a_{MgO}) of Wurtzite (WZ-) structure MgO [21]. As the MgO buffer layer thickness increases, the in-plane lattice constant decreases and saturates at the MgO layer thickness of 1.3 nm. The in-plane lattice constant for the thick MgO layers is 0.295 nm, which is almost equal to the in-plane lattice constant of Rock Salt (RS-) structure MgO ($a_{MgO}(\sqrt{2}$). The observed evolution of the in-plane lattice constant implies that the crystal structure of MgO changes with increasing layer thickness: Wurtzite structure for MgO thickness less than 0.8 nm; Rock Salt structure for MgO thickness larger than 1.3 nm. We note that Al_2MgO_4 (spinel structure) is not formed at the MgO/Al_2O_3 interface in our case, although the formation of Al_2MgO_4 (spinel structure) by interdiffusion between Al_2O_3 and MgO was reported [22]. The RHEED observation suggests the epitaxy relationship: ZnO(11–20)/RS-MgO(1–10)/WZ-MgO(11–20)/Al_2O_3(1–100).

ZnO layers were grown on MgO/c-Al_2O_3 with systematically varying the MgO buffer layer thickness. The growth rate of ZnO grown on MgO buffer thicker than 3 nm was about 1.5 times faster than that of ZnO grown on MgO buffer thinner than 2.7 nm. The difference in growth rate is likely due to inversion of polarity [23]. The growth rate of ZnO layer is limited by the sticking coefficient of Zn atoms under O-rich growth condition. The sticking coefficient of Zn-atoms on Zn-polar ZnO is larger than on O-polar ZnO because the surface O-atoms of Zn-polar ZnO have 3 dangling bonds, while the surface O-atoms of O-polar ZnO have just 1 dangling bond [23].

To precisely determine the crystal structure of the MgO and ZnO/MgO/c-Al_2O_3 interface, we carried out HRTEM observation. We chose 2 samples, one consisting of ZnO/3 nm-thick MgO/c-Al_2O_3 (Fig. 6(a)) which showed

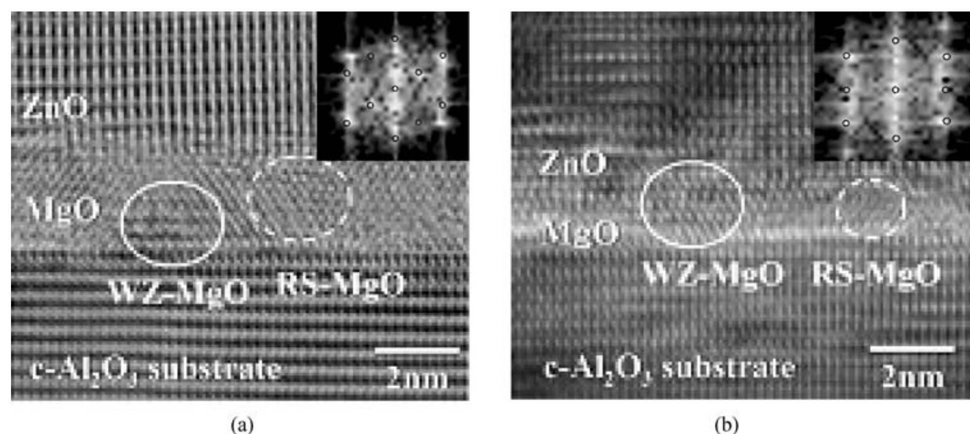

Fig. 6 HRTEM images of ZnO/MgO/Al_2O_3 heterostructure with the zone axis of ZnO[11–20]. (a) The thickness of MgO is 3 nm. Main part of the MgO layer consists of Rock Salt structure with a small mixture of Wurtzite structure. (b) The thickness of MgO is 1.5 nm. The MgO buffer consists of Wurtzite structure layer with small mixture of Rock Salt structure. The insets are FFT images of MgO buffer layers

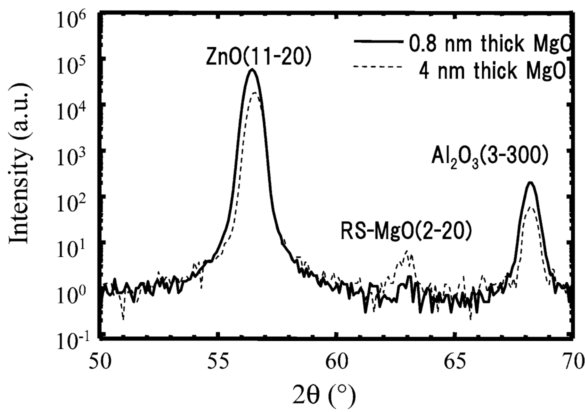

Fig. 7 2θ−ω GRIXRD for 30 nm-thick $ZnO/MgO/Al_2O_3$ structures. MgO layer thickness is (a) 0.8 nm, and (b) 4 nm

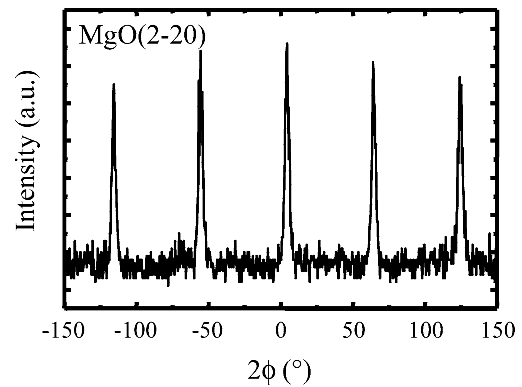

Fig. 8 ϕ scan for (2–20) diffraction from RS-MgO (2.5 nm thick) showing clear six-fold symmetry

Zn-polarity as will be indicated in the next section, and the other consisting of ZnO/1.5 nm-thick MgO/c-Al_2O_3 (fig. 6(b)) which showed O-polarity. Figure 6 shows HRTEM images with the zone axis of ZnO[11–20]. Figure 6(b) shows that the 1.5 nm-thick MgO buffer is single crystalline. The MgO buffer consists of Wurtzite structure layer as indicated by FFT analysis (Fig. 6(a)) with small mixture of Rock Salt structure. Figure 6(a) shows that the 3 nm thick MgO is also single crystalline. The main part of the MgO layer consists of Rock Salt structure as indicated by FFT analysis with a small mixture of Wurtzite structure. The HRTEM data show the epitaxy relationships: ZnO(11–20) RS-MgO(1–10)//WZ-MgO(11–20)//Al_2O_3(1–100). We note that these epitaxy relationships are the same as determined by RHEED observation.

Figure 7 shows 2θ−ω GRIXRD for 30 nm-thick $ZnO/MgO/Al_2O_3$ structures, where MgO layer thickness were (a) 0.8 nm, and (b) 4 nm. The diffraction peak at $2\theta = 63^\circ$ is assigned to RS-MgO (2–20) diffraction. Although the diffraction peak of WZ-MgO is masked by the diffraction peak of ZnO, the existence of RS-MgO is evident even in a thin 0.8 nm thick MgO layer. It is interesting to note that the in-plane lattice constant of MgO as measured by GRIXRD is not changed with layer thickness, which suggests that RS-MgO grown on WZ-MgO surffers from strain relaxation from the very beginning of growth. A ϕ scan for (2–20) diffraction from RS-MgO (2.5 nm thick) shows clear six-fold symmetry (Fig. 8). The epitaxy relationship is determined to be ZnO[11–20]// RS-MgO [1–10] //WZ-ZnO[11–20] //Al_2O_3[1–100] as revealed from the result of 2-axis measurement of GIXRD (Fig. 9), which is consistent with the RHEED and TEM investigation.

3.2.2 Characterization of polarity of ZnO films

To characterize the polarity of ZnO films, we carried out wet etching and CBED. In general, Zn-polar ZnO is more resistant to acid than O-polar ZnO [24]. The surface of O-polar ZnO is O-terminated, while Zn-polar ZnO surface is Zn-terminated [24, 25]. A charge transfer from Zn atoms to underlying O atoms occurs on a Zn-polar sirface due to the large electronegativity difference between Zn and O atoms [24, 26]. So, there are fewer electrons to react with H^+ in acid on the surface of Zn-polar ZnO. The etched rates of ZnO grown on 1.5 nm thick WZ-MgO buffer layer and 3 nm thick RS-MgO buffer layer were >130 nm/min and 23 nm/min, respectively. Thus, ZnO grown on 3 nm thick MgO buffer layer was Zn-polar while ZnO grown on 1.5 nm thick MgO buffer layer was O-polar.

Figure 10 shows the measured CBED pattern of ZnO grown on 3 nm thick MgO buffer layer and a simulated pattern of Zn-polar ZnO since the simulated CBED pattern of Zn-polar ZnO (Fig. 10(a)) closely matches the measured CBED pattern, we can conclude that Zn-polar ZnO grew on a 3 nm thick MgO buffer layer. Thus, it is clear that the MgO buffer layer thickness is crucial in determining the polarity of the subsequent ZnO layer.

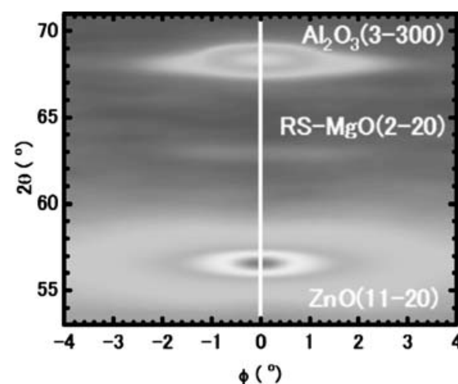

Fig. 9 2-axis GIXRD mapping. The epitaxy relationship is determined to be ZnO[11–20]// RS-MgO [1–10] //WZ-ZnO[11–20] //Al_2O_3[1–100]

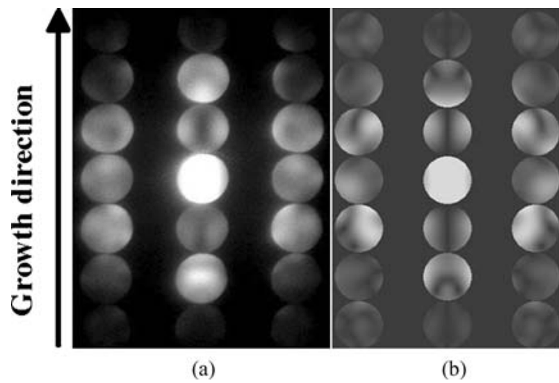

Fig. 10 (a) Measured CBED pattern of ZnO grown on 3 nm thick MgO buffer layer (b) Simulated pattern of Zn-polar ZnO

3.2.3 Atomic configuration at the ZnO/MgO/Al_2O_3 interface

Let us first consider why WZ-MgO is formed on O-terminated c-Al_2O_3. The ion radius (r_{ion}) of Al (r_{ion}) is 67.5 pm for 6-fold coordination as in Al_2O_3. The ion radius of Mg is 86 pm for 6-fold coordination, while 71 pm for 4-fold coordination. Considering the difference in ion radius between Al and Mg, MgO with 4-fold coordination (Wurtzite structure) would be more easily formed on c-Al_2O_3 in terms of ion-radius matching.

Figure 11 shows schematics of the ZnO/MgO/Al_2O_3 interface structure. When the thickness of MgO is thinner than 2.7 nm, WZ-MgO is formed. The polarity of WZ-MgO is considered to be O-polar like as O-polar ZnO grown directly on O-terminated Al_2O_3 [27]. Since the crystal polarity will be retained in the growth of the same crystal structure, the polarity of ZnO grown on O-polar MgO should be O-polar (Fig. 8(a)). As MgO becomes thicker than 3 nm, the crystal structure of MgO changes to RS-MgO. Since RS-MgO has an inversion symmetry, RS-MgO can invert the crystal polarity [28]. The underlying MgO layer is O-polar and the polarity of ZnO grown on RS-MgO will be changed to Zn-polar as schematically shown in Fig. 8(b). Similar mechanism for polarity inversion is proposed by Kato et al. [23].

4 Conclusion

We have succeeded in growing Ga-polar GaN epilayers on an NH_3 pre-exposed ZnO/MgO/c-sapphire template. The crystal polarity of the ZnO layer was confirmed by CBED, while that of the GaN layer was characterized by etching and CBED. An interface model for the Ga-polar GaN/O-polar ZnO is proposed, where a Zn_2N_3 layer was suggested to be formed during NH_3 pre-exposure.

We confirmed that we can control the polarity of ZnO layers grown on c-Al_2O_3 by varying MgO buffer layer thickness. ZnO grown on 3 nm or thicker MgO buffer layers is Zn-polar, and ZnO grown on 2.7 nm or thinner MgO buffer layer resulted in O-polar. Zn-polar ZnO showed about 1.5 times higher growth rate than O-polar ZnO.

From RHEED and TEM observations, it is revealed that the crystal structure of MgO buffer layers grown on c-Al_2O_3 substrates is changed with increasing MgO buffer layer thickness from Wurtzite to Rock Salt structure. Further more, GIXRD revealed that six-fold symmetry single domain RS-MgO was epitaxially grown on WZ-MgO with strain relaxation. The epitaxy relationship is ZnO[11–20]// RS-MgO[1–10] //WZ-ZnO[11–20] //Al_2O_3[1–100] revealed from the result of RHEED, HRTEM and 2-axis measurement of GIXRD. The origin of Wurtzite structure MgO is discussed in terms of difference of ion radius between Al and Mg. The polarity controlling mechanism of O-polar ZnO is, when the thickness of MgO is thinner than 2.7 nm, WZ-MgO is formed. The polarity of WZ-MgO is considered to be O-polar on O-terminated Al_2O_3, which resulted in O-polar ZnO on O-polar WZ-MgO. Since RS-MgO has an inversion symmetry, RS-MgO can invert crystal polarity. The underlying MgO layer

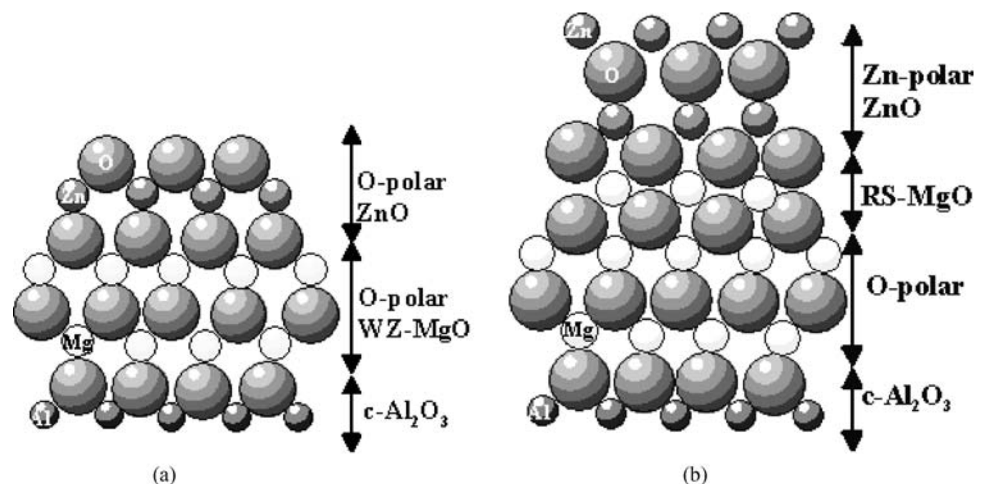

Fig. 11 Atomic configuration of ZnO/MgO/Al_2O_3 heterostructures. (a) The thickness of MgO is thinner than 2.7 nm, in which (b) $t_{MgO} \geq$ 3 nm, when the crystal structure of MgO is changed to RS-MgO

is O-polar and the polarity of ZnO grown on RS-MgO should be changed to Zn-polar. In conclusion, we can realize selective growth of Zn- or O-polar ZnO on c-Al_2O_3 without any especial ex-situ treatment by controlling MgO buffer layer thickness.

References

1. S. Nakamura, InGaN/GaN/AlGaN-based laser diodes grown on epitaxially laterally overgrown GaN. *J. Mater. Res.*, **14**, 2716 (1999).
2. S.T. Sheppard, K. Doverspike, W.L. Pribble, S.T. Allen, J.W. Palmour, L.T. Kehias, and T.J. Jenkins, High-power microwave GaN/AlGaN HEMTs on semi-insulating silicon carbide substrates. *IEEE Electron. Dev. Lett.*, **20**(4), 161 (1999).
3. D.M. Bagnall, Y.F. Chen, Z. Zhu, T. Yao, S. Koyama, M.Y. Shen, and T. Goto, *Appl. Phys. Lett.*, **70**, 2230 (1997).
4. Z.K. Tang, G.K.L. Wong, P. Yu, M. Kawasaki, A. Ohtomo, H. Koinuma, and Y. Segawa, *Appl. Phys. Lett.*, **72**, 3270 (1998).
5. D.M. Bagnall, Y.F. Chen, Z. Zhu, T. Yao, M.Y. Shen, and T. Goto, *Appl. Phys. Lett.*, **73**, 1038 (1998).
6. T. Detchprohm, K. Hiramatsu, H. Amano, and I. Akasaki, Hydride vapor phase epitaxial growth of a high quality GaN film using a ZnO buffer layer. *Appl. Phys. Lett.*, **61**, 2688 (1992).
7. A. Usui, H. Sunakawa, A. Sakai, and A. Yamaguchi, Thick GaN epitaxial growth with low dislocation density by hydride vapor phase epitaxy. *Jpn. J. Appl. Phys.*, **36**, 899 (1997).
8. X.Q. Shen, T. Ide, S.H. Cho, M. Shimizu, S. Hara, H. Okumura, S. Sonoda, and S. Shimizu, Essential change in crystal qualities of GaN films by controlling lattice polarity in molecular beam epitaxy. *Jpn. J. Appl. Phys.*, **39**, 16 (2000).
9. H. Okumura, M. Shimizu, X.Q. Shen, and T. Ide, Polarity control in MBE growth of III-nitrides, and its device application. *Curr. Appl. Phys.*, **2**, 305 (2002).
10. Y. Chen, S.K. Hong, H.J. Ko, V. Kirshner, H. Wenisch, T. Yao, K. Inaba, and Y. Segawa, Effects of an extremely thin buffer on heteroepitaxy with large lattice mismatch. *Appl. Phys. Lett.,* **78**, 3352 (2001).
11. S.K. Hong, H.J. Ko, Y.F. Chen, and T. Yao, *J. Vac. Sci. Technol. B*, **20**, 1656 (2002).
12. Y.F. Chen, S.K. Hong, H.J. Ko, V. Kirshner, H. Wenisch, T. Yao, K. Inaba, and Y. Segawa, *Appl. Phys. Lett.*, **78,** 3352 (2002).
13. Y. Chen, H.-J. Ko, S.-K. Hong, T. Yao, and Y. Segawa, *Appl. Phys. Lett.*, **80**, 1358 (2002).
14. T. Ohnishi, A. Ohtomo, M. Kawasaki, K. Takahashi, M. Yoshimoto, and H. Koinuma, *Appl. Phys. Lett.*, **72**, 824 (1998).
15. D. Li, M. Sumiya, S. Fuke, D. Yang, D. Que, Y. Suzuki, and Y. Fukuda, Selective etching of GaN polar surface in potassium hydroxide solution studied by X-ray photoelectron spectroscopy. *J. Appl. Phys.*, **90**, 4219 (2001).
16. K. Tuda and M. Tanaka, Refinement of crystal structural parameters using two-dimensional energy-filtered CBED patterns. *Acta Crystallogr*, **A55**, 939 (1999).
17. F. Vigué, P. Vennégués, S. Vézian, M. Laügt, and J.-P. Faurie, *Appl. Phys. Lett.*, **79**, 194 (2001).
18. V. Ramachandran, R.M. Feenstra, W.L. Samey, L. Salamancariba, J.E. Northrup, L.T. Romano, and D.W. Greve, Inversion of wurtzite GaN(0 0 0 1) by exposure to magnesium. *Appl. Phys. Lett.*, **75**, 808 (1999).
19. L.T. Romano, J.E. Northrup, A.J. Ptak, and T.H. Myers, Faceted inversion domain boundary in GaN films doped with Mg. *Appl. Phys. Lett.*, **77**, 2479 (2000).
20. S.K. Hong, T. Hanada, H.J. Ko, Y. Chen, T. Yao, D. Imai, K. Araki, M. Shinohara, K. Saitoh, and M. Terauchi, Control of crystal polarity in a wurtzite crystal. ZnO films grown on by plasma-assisted molecular-beam epitaxy on GaN. *Phys. Rev. B*, **65**, 115331 (2002).
21. W.R.L. Lambrecht, S. Limpijunmnong, and B. Segall, MRS Internet. *J. Nitride Semicond. Res.*, **4S1**, G6.8 (1999).
22. C.H. Lei, G.V. Tendeloo, J.G. Lisoni, M. Siegert, and J. Schubert, *J. Cryst. Growth*, **226**, 419 (2001).
23. H. Kato, K. Miyamoto, M. Sano, and T. Yao, *Appl. Phys. Lett.*, **84**, 4562 (2004).
24. J. Fryar, E. McGlynn, M.O. Henry, and A.A. Cafolla, *Physica B*, **340–342**, 210 (2003).
25. V. Staemmler, K. Fink, B. Meyer, D. Marx, M. Kunat, S. GilGirol, U. Burghaus, and Ch. Wöll, *Phys. Rev. Lett.*, **90**, 106102 (2003).
26. A.N. Mariano and R.E. Hanneman, *J. Appl. Phys.*, **34**, 384 (1963).
27. Y.F. Chen, H.J. Ko, S.K. Hong, T. Yao, and Y. Segawa, *Appl. Phys. Lett.*, **80**, 1358 (2002).
28. S.K. Hong, T. Hanada, H.J. Ko, Y.F. Chen, T. Yao, D. Imai, K. Araki, M. Shinohara, K. Saitoh, and M. Terauchi, *Phys. Rev. B*, **65**, 115331 (2002).